

Article

# Plasma–Chemical Hybrid NO<sub>x</sub> Removal in Flue Gas from Semiconductor Manufacturing Industries Using a Blade-Dielectric Barrier-Type Plasma Reactor

Haruhiko Yamasaki \* , Yuki Koizumi, Tomoyuki Kuroki and Masaaki Okubo

Department of Mechanical Engineering, Osaka Prefecture University, 1-1 Gakuen-cho, Naka-ku, Sakai, Osaka 599-8531, Japan

\* Correspondence: hyamasaki@me.osakafu-u.ac.jp; Tel.: +81-72-254-9233

Received: 28 June 2019; Accepted: 12 July 2019; Published: 16 July 2019



**Abstract:** NO<sub>x</sub> is emitted in the flue gas from semiconductor manufacturing plants as a byproduct of combustion for abatement of perfluorinated compounds. In order to treat NO<sub>x</sub> emission, a combined process consisting of a dry plasma process using nonthermal plasma and a wet chemical process using a wet scrubber is performed. For the dry plasma process, a dielectric barrier discharge plasma is applied using a blade-barrier electrode. Two oxidation methods, direct and indirect, are compared in terms of NO oxidation efficiency. For the wet chemical process, sodium sulfide (Na<sub>2</sub>S) is used as a reducing agent for the NO<sub>2</sub>. Experiments are conducted by varying the gas flow rate and input power to the plasma reactor, using NO diluted in air to a level of 300 ppm to simulate exhaust gas from semiconductor manufacturing. At flow rates of ≤5 L/min, the indirect oxidation method verified greater removal efficiency than the direct oxidation method, achieving a maximum NO conversion rate of 98% and a NO<sub>x</sub> removal rate of 83% at 29.4 kV and a flow rate of 3 L/min. These results demonstrate that the proposed combined process consisting of a dry plasma process and wet chemical process is promising for treating NO<sub>x</sub> emissions from the semiconductor manufacturing industry.

**Keywords:** nonthermal plasma; NO<sub>x</sub> reduction; PFC; sodium sulfide; wet scrubber; blade-barrier electrode; semiconductor manufacturing

## 1. Introduction

Since 1950, the semiconductor manufacturing industry has continued to grow, raising concerns about the increasing emissions of perfluorinated compounds (PFCs) [1]. PFCs are characterized by a very high global-warming potential, meaning that they produce a large environmental impact, even at low concentrations. As a result, the Kyoto Protocol (COP3) in 1997 set country-specific targets for reducing PFCs. In 2018, COP24 established guidelines for certain regulations on PFCs in developing countries, highlighting the urgency of the task of eliminating PFCs. Methods for eliminating PFC gas used in the semiconductor manufacturing industry include combustion methods, which burn the PFC gas together with such fuels as oil and natural gas to decompose it into hydrogen fluoride and carbon dioxide [2,3], and catalytic methods, which use catalysts to decompose the gas into hydrogen fluoride and carbon dioxide by means of the hydrolysis reaction [4,5]. The hydrogen fluoride generated during treatment is dealt with by dissolving it in water and processing it as hydrogen fluoride solution, or by causing it to react with calcium hydroxide to immobilize it as CaF<sub>2</sub> [6]. Because the catalytic and CaF<sub>2</sub> fixing methods are not suitable for large-scale treatment of PFCs, large-scale treatment facilities have used the combustion method followed by wastewater processing. In the combustion method, NO<sub>x</sub> (NO + NO<sub>2</sub>) is generated as a byproduct of the decomposition of the PFCs. NO<sub>x</sub>, which is generated mainly by the combustion of fuel, is a harmful substance that causes photochemical oxidation processes

and other chemical changes in the atmosphere and produces aerosols, such as nitric acid (HNO<sub>3</sub>), that cause acid rain. Selective catalytic reduction (SCR) is a common technique for processing NO<sub>x</sub>. In the combustion method, however, immediately after the PFCs are burned, a water spray is applied to dissolve the resulting hydrogen fluoride (HF) in water. The problem for SCR is that the water spray brings the target exhaust gas down to a normal temperature, at which the catalyst cannot be activated. Furthermore, the HF can sometimes poison the catalyst for the SCR [7,8], which poses a problem for the treatment of the NO<sub>x</sub> generated during processing of the PFCs.

Plasma–chemical methods that use nonthermal plasma have been proposed as a method of removing the NO<sub>x</sub> at low temperatures [9–14]. The plasma–chemical method oxidizes NO to NO<sub>2</sub> by using nonthermal plasma to promote oxidation, and then it applies a scrubber to reduce the NO<sub>2</sub> to N<sub>2</sub>. Our research group has achieved highly efficient removal of NO<sub>x</sub> through treatment by a combined process of indirect oxidation by nonthermal plasma together with a sodium sulfite (Na<sub>2</sub>SO<sub>3</sub>) scrubber [9–12]. Kim et al. have also achieved NO<sub>x</sub> removal efficiency of more than 80% using nonthermal plasma–chemical methods to treat the NO<sub>x</sub> discharged from semiconductor plants [15]. Comparing the NO<sub>x</sub> removal efficiency of two different reducing agents, Na<sub>2</sub>S and Na<sub>2</sub>SO<sub>3</sub>, Kim et al. found that Na<sub>2</sub>S was highly efficient at removing NO<sub>x</sub> at 1/10 the concentration of Na<sub>2</sub>SO<sub>3</sub> (0.1 mass%). Although the cost of using Na<sub>2</sub>S is approximately three times higher than that of using Na<sub>2</sub>SO<sub>3</sub>, using Na<sub>2</sub>S as the reducing agent suppresses the reaction of the exhaust gas with oxygen, making high-efficiency treatment of NO<sub>x</sub> possible at 1/10 concentration (0.1 mass%) and reducing the cost of treating NO<sub>x</sub> to one-third the cost of Na<sub>2</sub>SO<sub>3</sub> [15].

With respect to dielectric barrier discharge (DBD) plasma excitation, research has been conducted on the effect of changing the shape of the electrode on its DBD discharge characteristics and ozone-generating characteristics [16]. This research shows that the discharge energy efficiency and ozone generation efficiency are improved by using a multipoint electrode or trench electrode rather than a plate electrode. In concentric cylindrical plasma reactors, which are commonly used in environmental plasma processing, the high voltage is applied perpendicular to the direction of the gas flow, which means the voltage value imposes limits on the possible cross-sectional area or distance between electrodes. Parallelization is therefore required to increase the processing flow rate. However, in the blade-barrier electrode-based plasma reactor proposed in this study, the discharge direction is parallel to the gas flow, making it suitable for high-flow treatment of exhaust gas with no limit on the flow rate, and promising a highly efficient treatment of exhaust gas.

As mentioned above, previous studies have evaluated individual performance such as NO<sub>x</sub> reduction by chemical scrubber and NO oxidation by ozone generator, but the performance of the plasma-chemical hybrid technique has not been clarified. In the present study, a method for treating NO<sub>x</sub> is considered that combines the nonthermal plasma oxidation method at normal temperatures with a wet scrubber. For the plasma process, there are two different plasma oxidation methods: a direct oxidation method, which irradiates plasma directly into the exhaust gas, and an indirect oxidation method, which combines the exhaust with radical gas irradiated with plasma in the air. NO in the simulated exhaust gas is oxidized to NO<sub>2</sub> by using a blade-barrier electrode reactor as a plasma reactor, and then NO<sub>x</sub> reduction is performed by Na<sub>2</sub>S scrubber.

## 2. Principle

In this section, the principle underlying the removal of NO<sub>x</sub> by means of a combined process consisting of a dry plasma process using nonthermal plasma and wet chemical process using a wet scrubber is described. The nonthermal plasma causes some of the oxygen present in the air to change into ozone (which is an oxidizer) and oxygen radical (O). Although some of the NO is reduced to N<sub>2</sub> by the reactions indicated in Equations (1) and (2) [17], most of the NO is oxidized to NO<sub>2</sub> by the ozone and radical oxygen, as shown in Equations (3) and (4) [17],





where N and O are radicals, e<sup>-</sup> is an electron, M is the third-body substance, and N<sub>2</sub> and O<sub>2</sub> are molecules in the air. Reaction (4) proceeds in the presence of oxygen radicals in the plasma. Because the NO<sub>2</sub> obtained by oxidation reactions (3) and (4) is water-soluble, by using the Na<sub>2</sub>S scrubber after oxidation, the NO<sub>2</sub> is reduced to N<sub>2</sub> and Na<sub>2</sub>SO<sub>4</sub>, which are nontoxic and water-soluble. This reaction is shown in Equation (5).



### 3. Experimental Apparatus and Method

In this study, a blade-barrier electrode plasma reactor is used to generate ozone and radical oxygen for the purpose of oxidizing the NO, as shown in Equations (3) and (4). A schematic diagram of the blade-barrier plasma reactor and a detailed view of the blade electrode are shown in Figure 1. To increase the strength of the electric field, a multihole ( $\varphi 2 \times 16$ ) blade electrode is used. The gas flows from the top of the reactor, passes through the multihole blade electrode, and enters the discharge part. After the reaction in the discharge part, the gas flows out of the reactor through the holes in the lower electrode ( $\varphi 2 \times 4$ ). To elicit DBD discharge, a dielectric barrier made of acrylic is installed on the lower electrode. The upper electrode is equipped with 10 blades shaped like knife edges. The distance between the blades is 5.3 mm, the width of each blade is 1.5 mm, and the height is 11 mm. The two end blades are 35 mm in length, and the remaining eight blades are 50 mm in length. The upper and lower electrodes are 72.5 mm in diameter with a distance between the electrodes of 7 mm, including the thickness of the dielectric barrier.

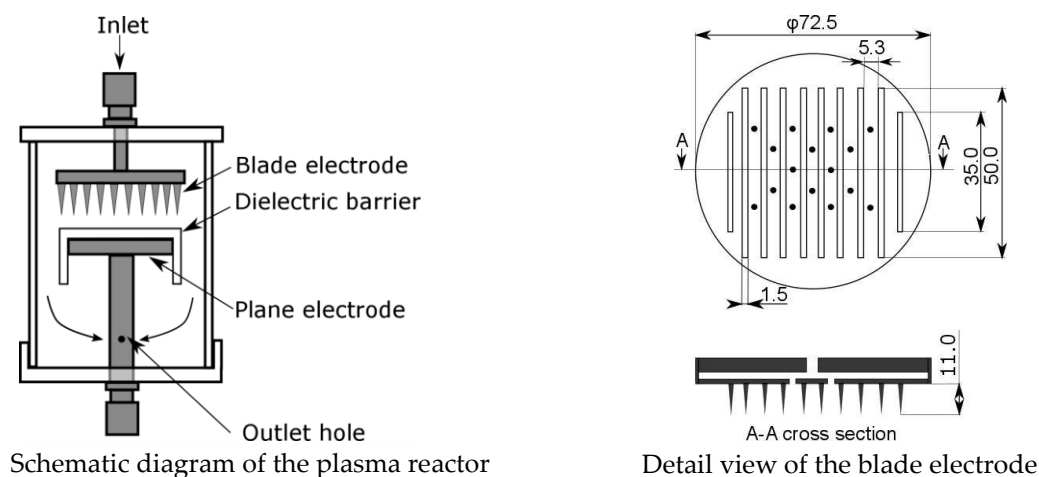


**Figure 1.** Schematic diagram of the plasma reactor and detail view of the blade electrode.

In this study, the practicality of the proposed NO<sub>x</sub> removal device is considered by two methods of NO<sub>x</sub> removal: direct oxidation and indirect oxidation. The direct oxidation method enables simulated exhaust gas to flow directly into the plasma reactor, where the nonthermal plasma directly irradiates the simulated exhaust gas, oxidizing the NO gas into NO<sub>2</sub>. A schematic diagram of the experimental setup for the direct plasma oxidation method is shown in Figure 2. The external air is compressed with a compressor, the fine particles are removed with a filter, and the moisture is removed with a desiccant to dry the air. The dry air is mixed with NO gas supplied from a gas cylinder (2%, N<sub>2</sub> balance), with the flow rate and concentration regulated by mass flow controllers. After the simulated exhaust gas is passed through the plasma reactor and irradiated with the nonthermal plasma, it is passed through a

heater at a flow rate of 3 L/min and heated to 270 °C to remove the O<sub>3</sub> that is generated in the plasma reactor. The remaining gas is then exhausted. After removal of the O<sub>3</sub>, the simulated exhaust gas passes through the reduction process by a bubble injection-type Na<sub>2</sub>S scrubber and then flows into a gas analyzer. The respective concentrations of NO, NO<sub>x</sub> (NO+NO<sub>2</sub>), CO, and N<sub>2</sub>O were measured with a gas analyzer (Horiba Co. Ltd., PG-240, Kyoto, Japan, chemiluminescence for NO, NO<sub>x</sub>, infrared absorption for CO and O<sub>2</sub> for zirconia method,) and N<sub>2</sub>O meter (Horiba Co. Ltd., VIA-510, Kyoto, Japan, infrared absorption for N<sub>2</sub>O). To ensure that the pressure inside the plasma reactor remained at atmospheric pressure during the experiment, the pressure was monitored upstream of the reactor. In this experiment, the concentration of NO was set at 300 ppm, and the total flow rate flowing into the reactor was changed to 3, 5, 10, and 15 L/min.

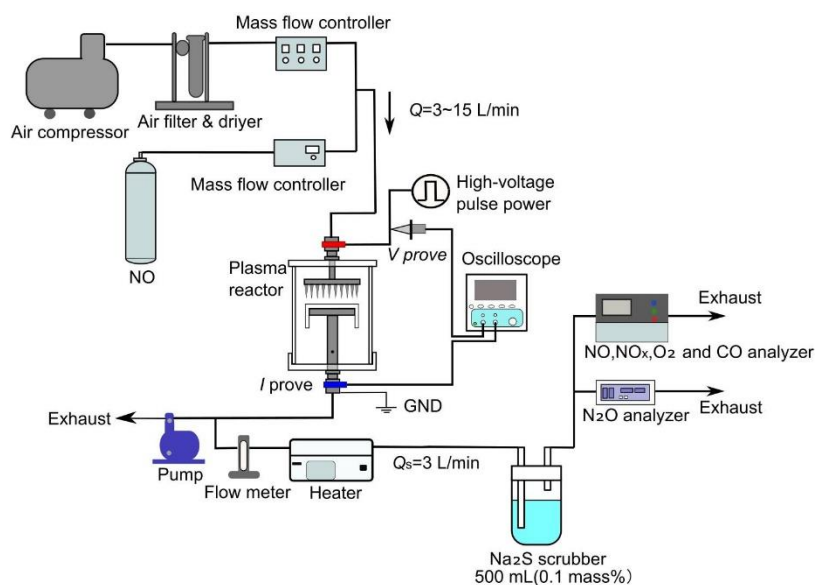


**Figure 2.** Schematic diagram of the experimental setup for direct plasma oxidation method.

A schematic diagram of the experimental setup for the indirect plasma oxidation method is shown in Figure 3. Unlike the direct plasma oxidation method, in which the simulated exhaust gas is directly irradiated with nonthermal plasma, in the indirect plasma oxidation method where only dry air flows through the reactor, and ozone is generated by irradiating this air with the nonthermal plasma. This ozone is then combined with the simulated exhaust gas to oxidize the NO in the gas to NO<sub>2</sub>. In the direct plasma oxidation method, when the exhaust gas is at a high temperature, the gas volume expands compared to room temperature. This decreases the residence time of the gas and reduces oxidation performance. In contrast, the indirect plasma oxidation method offers the advantage that the air is treated at normal temperatures, so the residence time does not change, and oxidation performance does not decrease. The external air is compressed with a compressor, the fine particles are removed with a filter, and the moisture is removed with a desiccant to dry the air. The dry air is branched, with one part going to the plasma reactor and the other part mixed with NO gas supplied from a gas cylinder (2%, N<sub>2</sub> balance). The dry air irradiated by the nonthermal plasma in the plasma reactor is combined with the simulated exhaust gas and then passed through the heater to remove the O<sub>3</sub>. The residence time of the mixture between the mixing point and the heater is 0.2–0.5 s. The residence time is enough time to react and mix NO with ozone since oxidation of NO is immediately occurred by ozone. Especially in this experiment, a tube with diameter of 4mm is used, which is quite small and considers that NO and ozone mix completely in the tube. In this experiment, the concentration of NO was set at 300 ppm and the flow rate of dry air flowing into the reactor at 1.0 L/min. The total flow rate of the air passing through the reactor and mixing with the exhaust gas was changed to 3, 5, 10, and 15 L/min.

The voltage applied to the plasma reactor was the same for the direct and indirect methods. An insulated gate bipolar transistor power supply was used to apply high-voltage pulses (max. 38 kV) at the following frequencies: 210, 420, 630, 840, and 1020 Hz. The discharge power in the plasma reactor was measured by an oscilloscope (Yokogawa Electric Corporation DL1740, Tokyo, Japan) using a high-voltage probe (Tektronix Co. Ltd., P6015A, Beaverton, USA) and an electric current probe (Tektronix Co. Ltd., P6021, Beaverton, USA). Figure 4 shows typical waveforms of the voltage, the current, and the product of the voltage and current as measured by the oscilloscope. To find the discharge power, the integral of the product of the voltage and current was calculated over one wavelength and then multiplied by the frequency. For the wet scrubber, sodium sulfide ( $\text{Na}_2\text{S}$ , 9-hydrate, Sigma-Aldrich, Japan Co. LLC, Tokyo, Japan) was used in an aqueous solution of 500 mL with an initial concentration of 0.1 mass%. Before processing, the pH was measured as  $11.9 \pm 0.2$ , and the oxidation-reduction potential (ORP) was measured as  $-300 \pm 20$  mV using a pH/ORP meter (Horiba Co. Ltd., D-53, Kyoto, Japan). The pH level requires careful attention because if it drops to less than 10, the  $\text{Na}_2\text{S}$  will react with the acid to generate highly toxic  $\text{H}_2\text{S}$  [18]. An  $\text{H}_2\text{S}$  detector (Honeywell International Inc., ToxiRAE3- $\text{H}_2\text{S}$ ) is therefore installed near the  $\text{Na}_2\text{S}$  scrubber vessel for the duration of the experiment to ensure that the pH would never drop to less than 10.

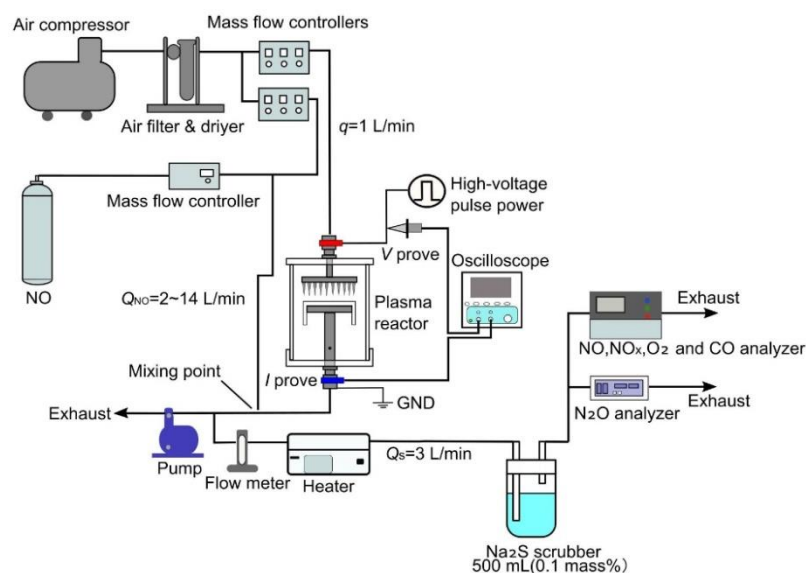


**Figure 3.** Schematic diagram of the experimental setup for indirect plasma oxidation method.

To evaluate the combined process of the dry plasma process and the wet chemical process using the wet scrubber, in this study  $\text{NO}_x$  concentrations at various discharge power are measured. Furthermore, NO conversion efficiency and  $\text{NO}_x$  removal energy efficiency are calculated and compared.

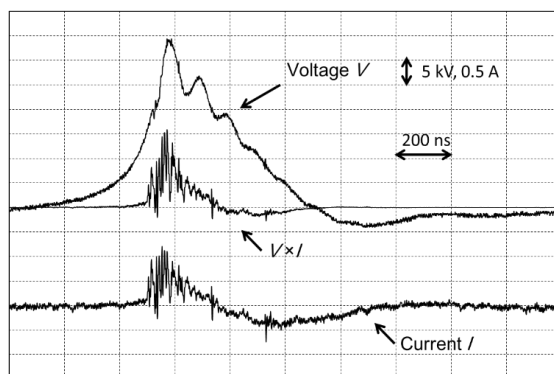


**Figure 4.** Waveform of voltage  $V$ , current  $I$  and instantaneous power  $V \times I$  in air +  $\text{NO}_x$  (300 ppm) at  $Q = 5$  L/min by the direct oxidation way. (horizontal axis: 200  $\mu\text{s}$  for 1 div, vertical axis: 5 kV and 0.5 A for 1 div).

#### 4. Results and Discussion

To evaluate the NO oxidation and removal characteristics of the treatment by the combined dry plasma and wet chemical processes using the direct oxidation method, the components of the treated gas relative to the discharge power are measured. Figure 5a–d show the gas concentrations after the combined process under each flow condition ( $Q = 3, 5, 10,$  and  $15$  L/min). From Figure 5a–d, it is seen that the NO decreased as the discharge power increased. Furthermore, as the NO decreased, the  $\text{NO}_2$  increased, causing a reduction in  $\text{NO}_x$  as the  $\text{NO}_2$  is removed by the  $\text{Na}_2\text{S}$  scrubber. In Figure 5a, as the discharge power rose from its initial value to 10.5 W ( $V_{p-p} = 25.6$  kV), the NO concentration decreased from 271 to 30 ppm, and the  $\text{NO}_x$  concentration decreased from 295 to 80 ppm. This represents an 89% reduction of NO and a 73% reduction of  $\text{NO}_x$ . In Figure 5b, when the discharge power was 9.0 W ( $V_{p-p} = 24.7$  kV), the NO was reduced by 75% and the  $\text{NO}_x$  by 62%. In Figure 5c, when the discharge power was 11.3 W ( $V_{p-p} = 26.6$  kV), the NO was reduced by 54% and the  $\text{NO}_x$  by 45%. In Figure 5d, when the discharge power was 10.1 W ( $V_{p-p} = 24.9$  kV), the NO was reduced by 47% and the  $\text{NO}_x$  by 40%. These results demonstrate that treatment by the combined dry plasma and wet chemical processes effectively reduce  $\text{NO}_x$ . In Figure 5a–d, CO and  $\text{N}_2\text{O}$  were each less than 10 ppm.

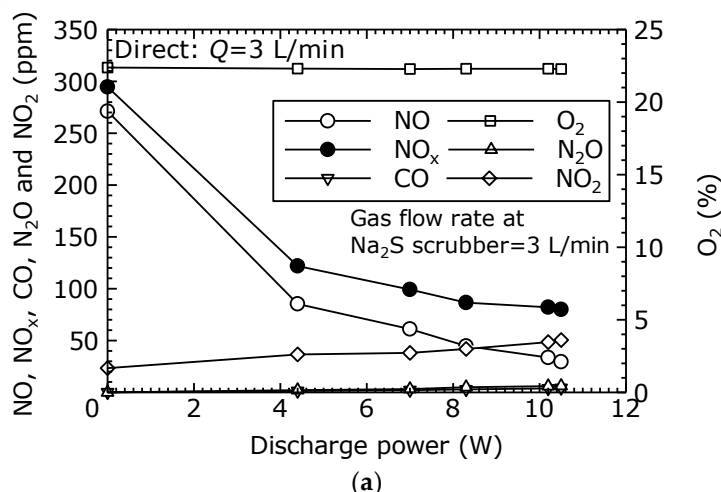


**Figure 5.** Cont.

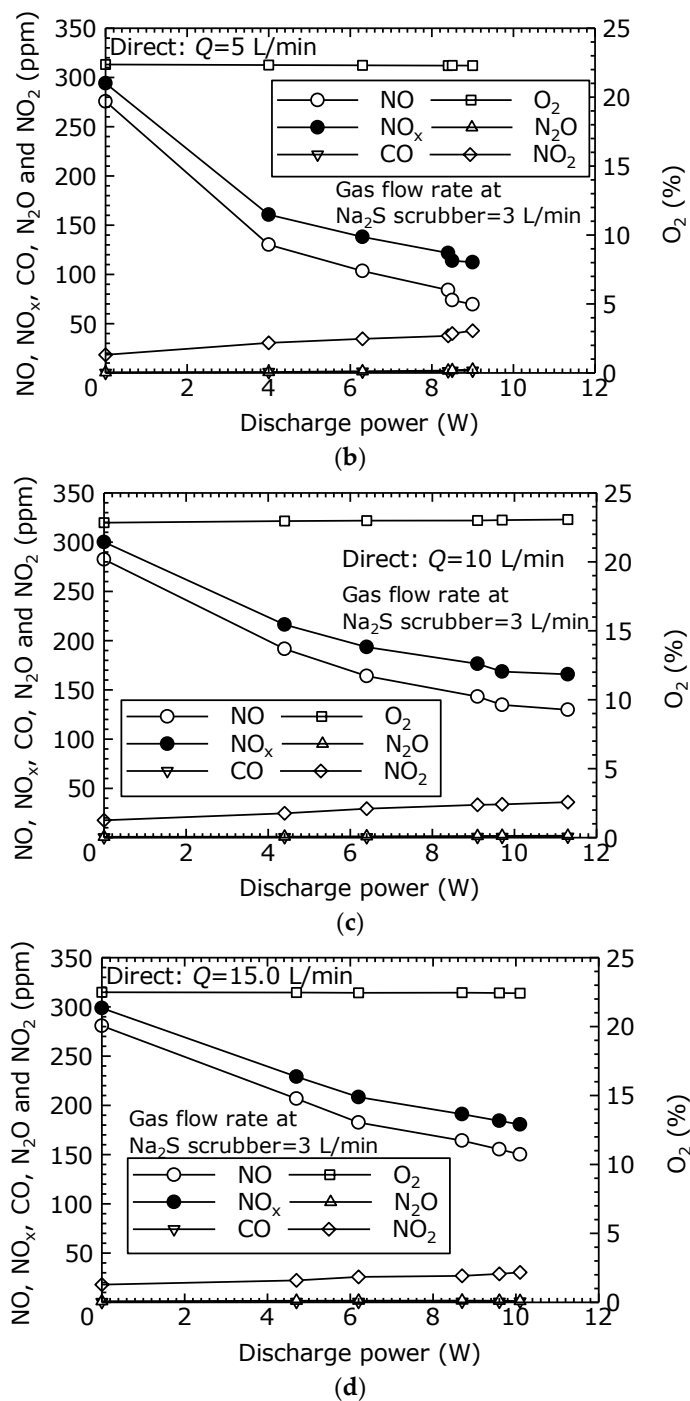


**Figure 5.** Gas concentrations in dry plasma and wet chemical processes by the direct oxidation method. ((a) Q = 3 L/min, (b) Q = 5 L/min, (c) Q = 10 L/min and (d) Q = 15 L/min).

The NO-to-NO<sub>2</sub> conversion characteristics of the dry plasma process are evaluated by the direct oxidation method. The relationship between the discharge power and the NO conversion efficiency at different flow rates is shown in Figure 6. In these experiments, the oxygen concentration was 22% to 24% at all flow rates. It is noted that NO<sub>2</sub> is produced at zero discharge power. It is known that a portion of NO converts to NO<sub>2</sub> upon coming into contact with oxygen by following reaction (2NO + O<sub>2</sub> → 2NO<sub>2</sub>). Figure 6 shows that the NO conversion efficiency increases with an increase in discharge power at any flow rate. It also shows that the NO conversion efficiency increased as the flow rate decreased. As the flow rate increased, it reduced the residence time of the simulated exhaust gas in the

plasma reactor, thereby decreasing the amount of oxidation promotion reactions shown in Equations (3) and (4).

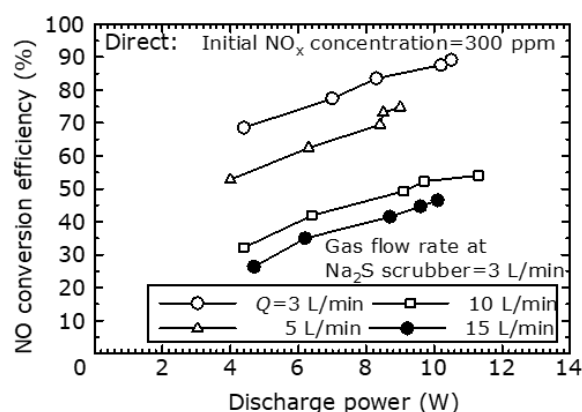


**Figure 6.** NO conversion efficiency varying with the discharge power at different flow rate by the direct oxidation method.

To evaluate the NO<sub>x</sub> removal characteristics of the combined dry plasma and wet chemical processes by the direct oxidation method, the NO<sub>x</sub> removal efficiency and NO<sub>x</sub> removal energy efficiency at different flow rates is shown in Figure 7. The actual gas flow rate into the scrubber was fixed at 3 L/min. Here, it was assumed that the full flow rate was processed. The NO<sub>x</sub> removal energy efficiency was calculated as the total flow rate relative to the NO<sub>x</sub> removal amount. Figure 7 shows that as the total flow rate increased, the NO<sub>x</sub> removal efficiency decreased, and the NO<sub>x</sub> removal energy efficiency increased. Furthermore, at each flow rate, as the NO<sub>x</sub> removal efficiency increased, the NO<sub>x</sub> removal energy efficiency decreased. This is because, as shown in Figure 6, the NO oxidation efficiency rises as the discharge power increases. Within the scope of this experiment, when the NO<sub>x</sub> removal efficiency is 60%, the NO<sub>x</sub> removal energy efficiency is approximately 20–25 g (NO<sub>2</sub>)/kWh.

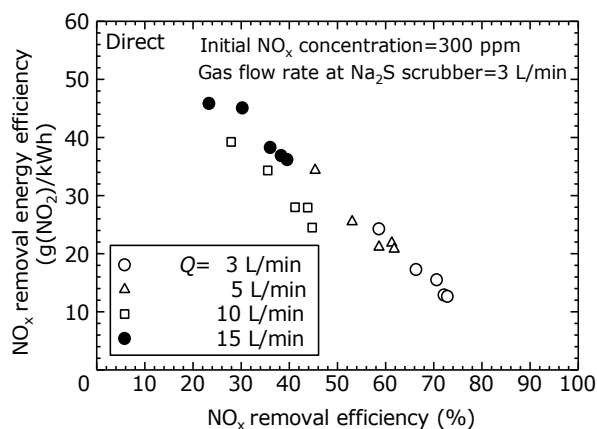


**Figure 7.** Measurement relation between NO<sub>x</sub> removal efficiency and NO<sub>x</sub> removal energy efficiency at different flow rate by the direct oxidation method. (The NO<sub>x</sub> removal energy efficiency is calculated as total flow rate  $Q = 3\text{--}15$  L/min from the inflow rate of exhaust gas to the chemical scrubber of  $Q_s = 3$  L/min).

Examining Figures 6 and 7 to evaluate the efficiency of the wet chemical process, the average ratio of the decrease in NO concentration to the decrease in NO<sub>x</sub> concentration is 89%, and the Na<sub>2</sub>S scrubber can reduce the NO<sub>2</sub> over 80%. At no time was the pH of the solution after treatment greater than 11. In addition, the ORP remained at or more than  $-263$  mV, and no H<sub>2</sub>S was detected.

In order to evaluate the NO oxidation and removal characteristics of the combined dry plasma and wet chemical processes using the indirect oxidation method, the components of the treated gas relative

to the discharge power was measured. Figure 8a–d shows the gas concentrations after the combined process under each flow condition ( $q = 1$  L/min,  $Q = 3, 5, 10$  and  $15$  L/min). From Figure 8a–d, it is seen that the NO decreased as the discharge power increased. Furthermore, as the NO decreased, the  $\text{NO}_2$  increased, causing a reduction in  $\text{NO}_x$  as the  $\text{NO}_2$  is removed by the  $\text{Na}_2\text{S}$  scrubber. In Figure 8a, as the discharge power rises from its initial value to  $6.6$  W ( $V_{p-p} = 25.8$  kV), the NO concentration decreased from  $281$  to  $7$  ppm, and the  $\text{NO}_x$  concentration decreased from  $298$  to  $52$  ppm. This represents a  $98\%$  reduction of NO and an  $83\%$  reduction of  $\text{NO}_x$ . In Figure 8b, when the discharge power is  $7.8$  W ( $V_{p-p} = 31.4$  kV), the NO is reduced by  $82\%$  and the  $\text{NO}_x$  by  $66\%$ . In Figure 8c, when the discharge power is  $8.3$  W ( $V_{p-p} = 26.0$  kV), the NO is reduced by  $43\%$  and the  $\text{NO}_x$  by  $36\%$ . In Figure 8d, when the discharge power is  $8.1$  W ( $V_{p-p} = 27.2$  kV), the NO is reduced by  $36\%$  and the  $\text{NO}_x$  by  $32\%$ . These results demonstrate that, using the indirect oxidation method as well, treatment by the combined dry plasma and wet chemical processes effectively reduce  $\text{NO}_x$ . In Figure 8a–d, CO and  $\text{N}_2\text{O}$  are each less than  $10$  ppm.

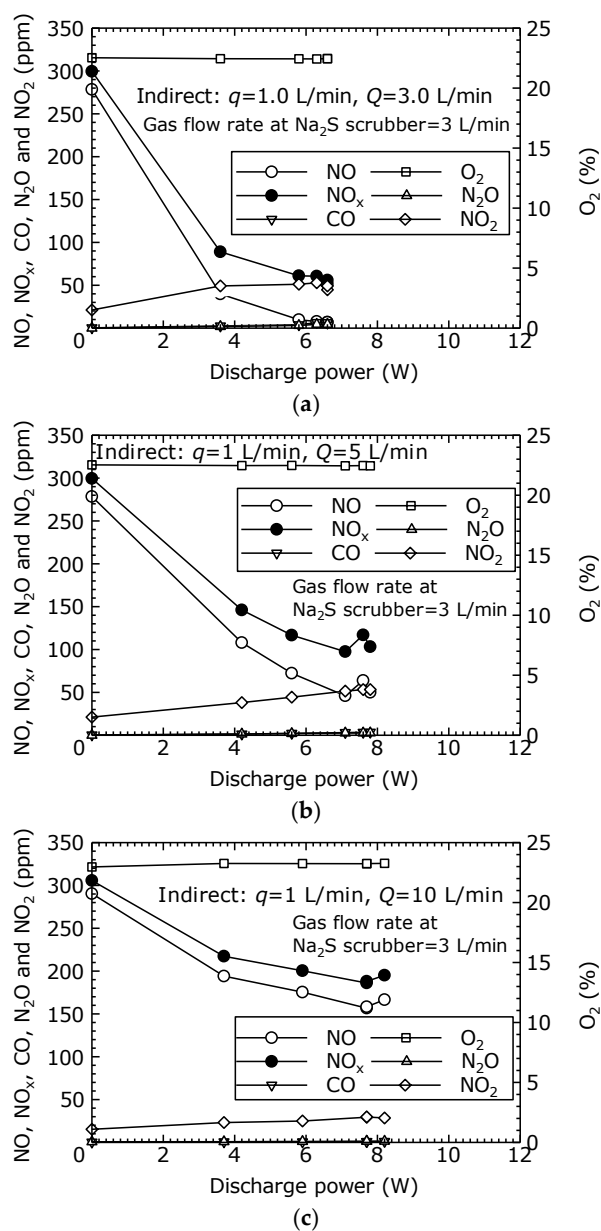
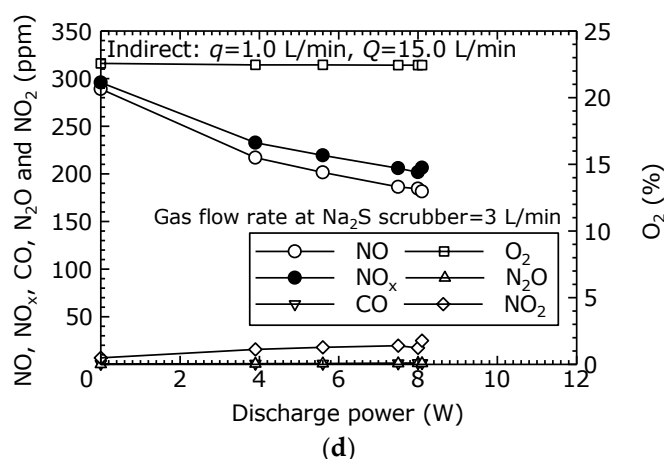
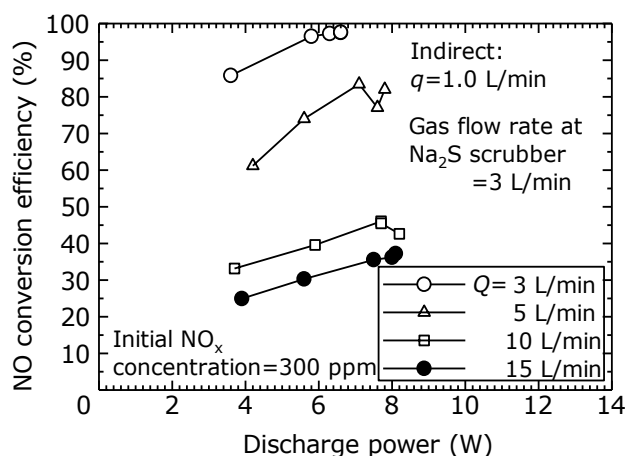


Figure 8. Cont.



**Figure 8.** Gas concentrations in dry plasma and wet chemical processes by the indirect oxidation method. ((a)  $Q = 3$  L/min, (b)  $Q = 5$  L/min, (c)  $Q = 10$  L/min and (d)  $Q = 15$  L/min).

In order to evaluate the NO to NO<sub>2</sub> conversion characteristics of the dry plasma process by the indirect oxidation method, the relationship between the discharge power and the NO conversion efficiency at different flow rates is shown in Figure 9. In these experiments, the oxygen concentration was 22% to 24% at all flow rates. In the indirect oxidation method, even if the total flow rate is changed, the flow rate into the plasma reactor was constant ( $Q = 1$  L/min), which means the ozone generated in the plasma reactor stayed constant regardless of the total flow rate. Therefore, as shown in Figure 9, the NO conversion efficiency varies by roughly the same magnitude as the flow rate ( $Q - q$ ), which is the total flow rate  $Q$  minus the flow rate  $q$  flowing into the plasma reactor. However, when the total flow rate was low, the ozone might be used for further oxidation of NO<sub>2</sub>, which suggests that an optimal flow rate may exist. In this experiment, as the flow rate increased, the NO conversion efficiency decreased, but the production of CO and N<sub>2</sub>O was suppressed.



**Figure 9.** NO conversion efficiency varying with the discharge power at different flow rate by the indirect oxidation method.

To evaluate the NO<sub>x</sub> removal characteristics of the dry plasma and wet chemical processes by the direct oxidation method, the NO<sub>x</sub> removal efficiency and NO<sub>x</sub> removal energy efficiency at different flow rates is shown in Figure 10. The NO<sub>x</sub> removal energy efficiency was evaluated based on the molecular mass of NO<sub>2</sub> per discharge power with the unit of g(NO<sub>2</sub>)/kWh. The actual gas flow rate into the scrubber was fixed at 3 L/min. Here, it is assumed that the full flow rate is processed. The NO<sub>x</sub> removal energy efficiency was calculated as the total flow rate relative to the NO<sub>x</sub> removal amount.

Figure 10 shows that, as the flow rate increased, the  $\text{NO}_x$  removal efficiency decreased, and the  $\text{NO}_x$  removal energy efficiency increased. As shown in Figure 10, it is clear that the flow rate affects the relationship between the  $\text{NO}_x$  removal efficiency and the  $\text{NO}_x$  removal energy efficiency. In the indirect oxidation method, the flow rate into the plasma reactor is constant at  $q = 1 \text{ L/min}$ , which means the ozone and radical oxygen produced stay constant, regardless of the total flow rate. This explains why the energy efficiency of  $\text{NO}_x$  removal varies for each flow rate. Within the scope of this experiment, when the  $\text{NO}_x$  removal efficiency was 80%, the  $\text{NO}_x$  removal energy efficiency was approximately 22–25  $\text{g}(\text{NO}_2)/\text{kWh}$ .

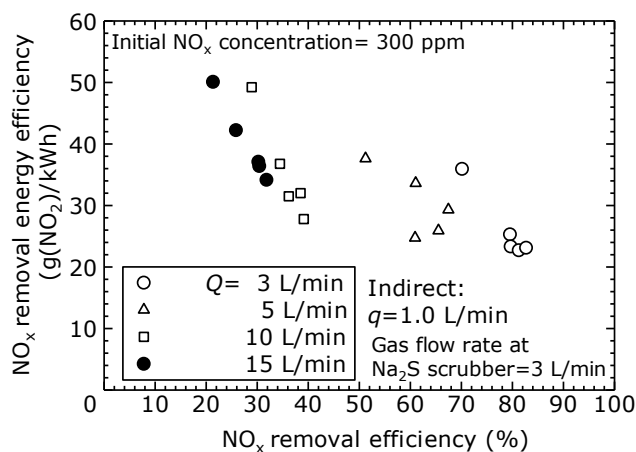


**Figure 10.** Measurement relation between  $\text{NO}_x$  removal efficiency and  $\text{NO}_x$  removal energy efficiency at different flow rate by the indirect oxidation method. (The  $\text{NO}_x$  removal energy efficiency is calculated as total flow rate  $Q = 3\text{--}15 \text{ L/min}$  from the inflow rate of exhaust gas to the chemical scrubber of  $Q_s = 3 \text{ L/min}$ ).

Examining Figures 9 and 10 to evaluate the efficiency of the wet chemical process, it is observed that the average ratio of the decrease in  $\text{NO}$  concentration to the decrease in  $\text{NO}_x$  concentration is 85%, and the  $\text{Na}_2\text{S}$  scrubber can reduce the  $\text{NO}_2$  over 80%. At no time was the pH of the solution after treatment greater than 11. In addition, the ORP remained at or more than  $-233 \text{ mV}$ , and no  $\text{H}_2\text{S}$  was detected.

To compare the efficiency of  $\text{NO}_x$  removal using the direct and indirect oxidation methods in this experiment, the relationship between the  $\text{NO}_x$  removal efficiency and the specific energy (SE) per unit flow rate is shown in Figure 11. The SE is calculated based on the total flow rate (3–15 L/min). The solid line is a trendline calculated by the least-squares method. Figure 11 shows no difference between the direct and indirect oxidation methods at SEs less than 50 J/L, when the  $\text{NO}_x$  removal efficiency is 20–40%. Although the indirect oxidation method generates a certain amount of ozone in the reactor regardless of the total flow rate, in this experiment, the amount of ozone generated by the indirect oxidation method is not enough to oxidize the  $\text{NO}$  in the simulated exhaust gas at the high flow rate (of 10 and 15 L/min). As the SE exceeds 50 J/L, the efficiency of  $\text{NO}_x$  removal by indirect oxidation increases, achieving an 80% removal efficiency at an SE of 132 J/L. It is considered that the amount of ozone generated by indirect oxidation method is larger than that of the direct oxidation method due to the increase of residence time as mentioned above.

These results demonstrate that the combined process of the dry plasma process using the indirect oxidation method and the wet scrubber process can remove  $\text{NO}_x$  with greater efficiency and energy savings. The plasma dry etching process used in the semiconductor industry requires a high-frequency voltage power supply and consumes several hundred to 1000 W of power. Because the power associated with the  $\text{NO}_x$  processing performed in this study was less than 10 W, the electricity consumption costs are very low. For example, assuming a  $2 \text{ m}^3/\text{min}$  exhaust class semiconductor plant that discharges  $\text{NO}_x$  at  $25 \text{ g}(\text{NO}_2)/\text{h}$ , the plasma power costs required to achieve 80% or greater  $\text{NO}_x$  removal using the

proposed system at a  $\text{NO}_x$  removal energy efficiency of  $25 \text{ g}(\text{NO}_2)/\text{kWh}$  would be very economical at  $\$0.20/\text{h}$  (assuming  $\$0.20/\text{kWh}$ ). There is a risk that  $\text{H}_2\text{S}$  may occur as a byproduct of using  $\text{Na}_2\text{S}$  as the chemical scrubber. However, by maintaining the pH at a sufficiently high value, it is possible to reduce  $\text{NO}_x$  using  $\text{Na}_2\text{S}$  at a third of the cost of using  $\text{Na}_2\text{SO}_3$ . In the actual semiconductor manufacturing, the concentration of  $\text{NO}_x$  is emitted  $100 \text{ ppm}$  at  $2000 \text{ L/min}$  [15]. The mass flow rate is much larger than in our experiment (maximum  $15 \text{ L/min}$ ). Since our experiment is fundamental research to remove  $\text{NO}_x$  at room temperature and atmospheric pressure, practical research should be performed for realizing development. The combined dry plasma and wet chemical processes can therefore be expected to serve as a low-cost and highly efficient method for treating  $\text{NO}_x$  emissions from the semiconductor manufacturing industry.

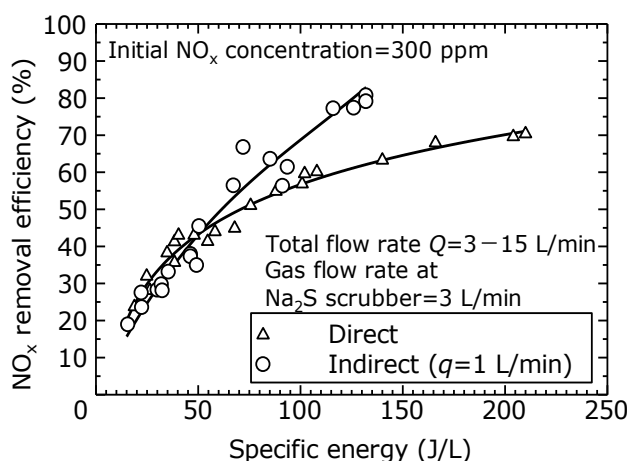


**Figure 11.**  $\text{NO}_x$  removal efficiency with direct and indirect oxidation method with respect to specific energy.

## 5. Conclusions

In this research,  $\text{NO}_x$  removal in simulate exhaust gas from semiconductor manufacturing is performed by a combined process of a direct/indirect DBD plasma process and a wet chemical process using a  $\text{Na}_2\text{S}$  scrubber. The research results contribute treatment  $\text{NO}_x$  emissions from the semiconductor manufacturing industry. We obtained the following results:

1. When the direct oxidation method was used, a maximum  $\text{NO}$  conversion rate of 89% and a  $\text{NO}_x$  removal rate of 73% at 25.6 kV and a flow rate of 3 L/min was achieved. When the indirect oxidation method was used, maximum  $\text{NO}$  conversion rate of 98% and a  $\text{NO}_x$  removal rate of 83% at 29.4 kV and a flow rate of 3 L/min was achieved. Although the  $\text{N}_2\text{O}$  and  $\text{CO}$  are detected as byproducts, they are less than 10 ppm in this experiment.
2. In the case used direct oxidation method, the  $\text{NO}_x$  removal energy efficiency was  $10\text{--}25 \text{ g}(\text{NO}_2)/\text{kWh}$  with  $\text{NO}_x$  removal efficiency of 60%. In the case used indirect oxidation method, the  $\text{NO}_x$  removal energy efficiency is  $20\text{--}25 \text{ g}(\text{NO}_2)/\text{kWh}$  with  $\text{NO}_x$  removal efficiency of 80%.
3. As results comparing the  $\text{NO}_x$  removal efficiency with the specific energy, when the specific energy was more than 50 J/L, the indirect oxidation method exhibited greater removal efficiency than the direct oxidation method, achieving a maximum  $\text{NO}_x$  removal efficiency of 83% at the specific energy of 132 J/L.
4. In the  $\text{NO}_x$  reduction process by  $\text{Na}_2\text{S}$  scrubber,  $\text{NO}_x$  reduction efficiency more than 80% was achieved. In this experimental range, at no time was the pH of the solution after treatment greater than 11. In addition, no  $\text{H}_2\text{S}$  was detected.

**Author Contributions:** H.Y., Y.K., T.K., and M.O. performed the data processing; H.Y., T.K., and M.O. conceptualized the ideas, developed the methodology. H.Y. and Y.K. performed the experimental activity; H.Y. prepared the original draft of the manuscript; T.K. and M.O. supervised the study, reviewed the original draft.

**Funding:** This study is partially supported by JSPS KAKENHI Grant No. 17H03498.

**Conflicts of Interest:** The authors declare no conflict of interest.

## References

1. Purohit, P.; Lsaksson, L.H. Global emissions of fluorinated greenhouse gases 2005–2050 with abatement potentials and costs. *Atmos. Chem. Phys.* **2017**, *17*, 2795–2816. [[CrossRef](#)]
2. Qin, L.; Han, J.; Wang, G.; Kim, H.J.; Kawaguchi, I. Highly efficient decomposition of CF<sub>4</sub> gases by combustion. *Sci. Res. Conf. Environ. Pollut. Public Health* **2010**, 126–130.
3. Chang, M.B.; Chang, J.S. Abatement of PFCs from semiconductor manufacturing processes by nonthermal plasma technologies: A Critical Review. *Ind. Eng. Chem. Res.* **2006**, *45*, 4101–4109. [[CrossRef](#)]
4. Lai, S.Y.; Pan, W.; Ng, C.F. Catalytic hydrolysis of dichlorodifluoromethane (CFC-12) on unpromoted and sulfate promoted TiO<sub>2</sub>-ZrO<sub>2</sub> mixed oxide catalysts. *Appl. Catal. B* **2000**, *45*, 207–217. [[CrossRef](#)]
5. Takita, Y.; Morita, C.; Ninomiya, M.; Wakamatsu, H.; Ishihara, T. Catalytic decomposition of CF<sub>4</sub> over AlPO<sub>4</sub>-based catalysts. *Chem. Lett.* **1999**, *28*, 417–418. [[CrossRef](#)]
6. Yasui, S.; Shoji, T.; Inoue, G.; Koike, K.; Takeuchi, A.; Iwasa, Y. Gas-solid reaction properties of Fluorine compounds and solid adsorbents for off-gas treatment from semiconductor facility. *Int. J. Chem. Eng.* **2012**, *2012*, 9. [[CrossRef](#)]
7. Xu, X.F.; Jeon, J.Y.; Choi, M.H.; Kim, H.Y.; Choi, W.C.; Park, Y.K. A strategy to protect Al<sub>2</sub>O<sub>3</sub>-based PFC decomposition catalyst from deactivation. *Chem. Lett.* **2005**, *34*, 364–365. [[CrossRef](#)]
8. Wang, Y.F.; Wang, L.C.; Shih, M.L.; Tsai, C.H. Effects of experimental parameters on NF<sub>3</sub> decomposition fraction in an oxygen-based RF plasma environment. *Chemosphere* **2004**, *57*, 1157–1163. [[CrossRef](#)] [[PubMed](#)]
9. Yamamoto, T.; Okubo, M.; Nagaoka, T.; Hayakawa, K. Simultaneous removal of NO<sub>x</sub>, SO<sub>x</sub> and CO<sub>2</sub> at elevated temperature using a plasma-chemical hybrid process. *IEEE Trans. Ind. Appl.* **2002**, *38*, 1168–1173. [[CrossRef](#)]
10. Fujishima, H.; Tatsumi, A.; Kuroki, T.; Tanaka, A.; Otsuka, K.; Yamamoto, T.; Okubo, M. Improvement in NO<sub>x</sub> removal performance of the pilot-scale boiler emission control system using an indirect plasma-chemical process. *IEEE Trans. Ind. Appl.* **2010**, *46*, 1722–1729. [[CrossRef](#)]
11. Fujishima, H.; Kuroki, T.; Ito, T.; Otsuka, K.; Yamamoto, T.; Yoshida, K.; Okubo, M. Performance characteristics of pilot-scale indirect plasma and chemical system used for the removal of NO<sub>x</sub> from boiler emission. *IEEE Trans. Ind. Appl.* **2010**, *46*, 1707–1714. [[CrossRef](#)]
12. Yamamoto, Y.; Yamamoto, H.; Takada, D.; Kuroki, T.; Fujishima, H.; Okubo, M. Simultaneous removal of NO<sub>x</sub> and SO<sub>x</sub> from flue gas of a glass melting furnace using a combined ozone injection and semi-dry chemical process. *Ozone Sci. Eng.* **2016**, *38*, 211–218. [[CrossRef](#)]
13. Chang, M.B.; Lee, H.M.; Wu, F.; Lai, C.R. Simultaneous removal of nitrogen oxide/nitrogen dioxide/sulfur dioxide from gas streams by combined plasma scrubbing technology. *J. Air Waste Manag. Assoc.* **2004**, *54*, 941–949. [[CrossRef](#)] [[PubMed](#)]
14. Han, B.; Kim, H.J.; Kim, Y.J. Removal of NO and SO<sub>2</sub> in a cylindrical water-film pulse corona discharger. *IEEE Trans. Ind. Appl.* **2005**, *51*, 679–684. [[CrossRef](#)]
15. Kim, H.J.; Han, B.; Woo, C.G.; Kim, Y.J. NO<sub>x</sub> removal performance of a wet reduction scrubber combined with oxidation by an indirect DBD plasma for semiconductor manufacturing industries. *IEEE Trans. Ind. Appl.* **2018**, *54*, 6401–6407. [[CrossRef](#)]
16. Takaki, K.; Hatanaka, Y.; Arima, K.; Mukaigawa, S.; Fujiwara, T. Influence of electrode configuration on ozone synthesis and microdischarge property in dielectric barrier discharge reactor. *Vacuum* **2009**, *83*, 128–132. [[CrossRef](#)]

17. Malik, M.A. Nitric oxide production by high voltage electrical discharge for medical uses: A review. *Plasma Chem. Plasma Process.* **2016**, *36*, 737–766. [[CrossRef](#)]
18. Mok, Y.S. Absorption reduction technique assisted by ozone injection and sodium sulfide for NO<sub>x</sub> removal from exhaust gas. *Chem. Eng. J.* **2006**, *118*, 63–67. [[CrossRef](#)]



© 2019 by the authors. Licensee MDPI, Basel, Switzerland. This article is an open access article distributed under the terms and conditions of the Creative Commons Attribution (CC BY) license (<http://creativecommons.org/licenses/by/4.0/>).